Atomistic Process and Simulation in the Regime of sub-50nm Gate Length

Ohseob Kwon, Kidong Kim, Jihyun Seo, and Taeyoung Won

Department of Electrical Engineering, School of Engineering, Inha University
253 Yonghyun-dong, Nam-gu, Incheon, Korea 402-751, E-mail: kos@hsel.inha.ac.kr

ABSTRACT

In this paper, we report an atomistic simulation approach for sub-50nm gate length FETs. The proposed atomistic approach consists of the coupling the molecular dynamics (MD) simulations of the collision cascades for ion implantation process and Kinetic Monte Carlo (KMC) simulations for the subsequent diffusion process. The impurity profiles from the MD and KMC calculations were interfaced with the quantum-mechanical device simulations. The device performance of FinFET with 20nm physical gate length is discussed in this paper.

Keywords: molecular dynamics, kinetic monte carlo, ion implantation, diffusion, device modeling, FinFET

1 INDRODUCTION

Recently, a great deal of attractions have been made on the development of novel nano-scale devices for sub-50nm gate length, such as double-gate (DG) MOSFET, vertical replacement-gate (VRG) MOSFET, ultra thin body (UTB) MOSFET, and FinFET [1-4]. These devices demand new modeling methodology for the simulations, i.e. an atomistic and quantum mechanical (QM) scheme.

In this paper, we report a simulation method based on atomistic approach for sub-50nm gate length. Molecular dynamics (MD) is implemented for the ion implantation process to form ultra-shallow junctions [5-6]. Thereafter, the diffusion process is simulated by using Kinetic Monte Carlo (KMC) with the damages and impurities distribution from the ion implantation profile in MD [7]. A device simulation is performed by using profiles from the results of KMC. As an exemplary case, we chose a FinFET structure with 20nm physical gate length. Let us start with a discussion of the simulation model (Section 2), followed by presentation of the results and discussion (Section 3).

2 SIMULATION MODEL

The concentration distribution of dopants during the ion implantation is calculated from the MD module. The MD approach accurately calculates the concentration distribution of dopants in the ion implantation using the recoil ion approximation (RIA). MD simulations can calculate range profiles of different ion species implanted into crystalline Si for nano-scale devices in ultra low energy regime. In our work, MD with a damage model has been employed. In order to model the ultra shallow junction, we used a modified RIA for dose-dependent damage. The Ziegler-Biersack-Littmark (ZBL) potential model, Eq. (1), has been used for the interaction among atoms. In order to model the electronic stopping power, the density functional theory by Echenique et al [8] was implemented in this work. Furthermore, the Firsov model was employed in order to model the energy loss during the inelastic collisions [9].

$$E_{ZBL} = V(r_{ij}) = \frac{Z_1 Z_2 e^2}{R_{ij}} \sum_{k=1}^{4} c_k \exp(-d_k \frac{r_{ij}}{a}), \qquad (1)$$

For an accurate atomic-scale model for diffusion of intrinsic point defects (I, V) and impurities (B) in ion-implanted silicon, we used a Kinetic Monte Carlo (KMC) method. In this type of KMC model, point defects and dopants are treated at an atomic scale while they are considered to diffuse in accordance with the reaction rates, which are given as input parameters [10]. These input parameters can be obtained from either first-principles calculations, classical MD simulation, or experimental data. Especially, the formation of clusters and extended defects, which usually control the annealing kinetics after ion implantation, should be minimized in the range of low dose in an effort to create dilute concentrations of I and V. Therefore, a simple kick-out mechanism has been tested and a good agreement with the experimental data [11] was verified in this condition. However, a more recent model, interstitialcy mechanism, is preferred when compared to the traditional kick-out mechanism by *ab initio* molecular dynamics [12].

We propose an atomistic diffusion mechanism involving fast-migrating intermediate species of the form. The reactions X_s + I ⇔ X_m and I + V ⇔ 0 are essentially diffusion limited, with capture radius of second neighbor atomic length (3.84Å) and direction of particle migration is limited to six neighbor sites. Here X_s is the immobile substitution impurity, which through reaction with a self-interstitial (I) forms a fast-migrating species X_m, which diffuse at a rate D_m. Ordinary, the diffusion rate is form in Arrhenius type ($D_0\exp(-E_{act}/KT)$). KMC simulations are performed by using the damage profiles and defects distribution from the MD simulations. The KMC is an event-driven technique, i.e., simulate events at random with probabilities according to the corresponding event rates. In this way, it self-adjusts the reasonable time step as the simulation proceeds. In our work, the only event that a

point defect (I,V) can perform is a jump. Their jump rate is given by Eq. (2).

$$J_{rate} = 6 \times D_0 \times exp(-R_m / kT) / \lambda^2 , \qquad (2)$$

The change of the transition probability density, *f(t)* over some short time interval, *dt* is proportional to the uniform transition probability, *r*, *dt*, and *f* because *f* gives the probability density that the object still remains at time *t*. The solution is given by Eq. (4) with boundary conditions. There, the simulation time is updated with $t' = t + \Delta t$ according to event hopping rate, Eq. (5).

$$df(t) = -rf(t)dt , \qquad (3)$$

$$f(t) = re^{-rt} , f(0) = r , \qquad (4)$$

$$\Delta t = -\frac{\log u}{R} , \qquad (5)$$

For the device of sub-50nm gate length, the nonlinear Poisson, Eq. (6) and Schödinger equation, Eq. (7) solved by using a finite different method (FDM) with Gunter's grid in self-consistent manner, followed by solving the continuity equation, Eq. (8) for current density. For QM solution, an iterative procedure is employed.

3 RESULTS AND DISCUSSION

In MD simulation, all simulations were performed on a Si {100} target at 300K. Dopants and damage profiles were simulated for B and As ions with the dose 1×10^{14} ions/cm^2. Fig.1 and Fig. 2 show the simulation results with the energy of 0.5, 1, 2, 4, 8, and 16 keV B implant into Si, respectively. As boron ion dose increases, local damage accumulation affects dopant distribution in the cases of ultra-low energy ion implantation. In other words, the channeling tail drops very steeply with dose increase. In case of As ion, the channeling tail drops very steeply with depth due to large atomic mass of the arsenic ion. Fig. 3 shows 3D distribution with the energy of 5 keV B implant into Si after 4,000 B ion. In this simulation, the mean range is 741.31 ?, and the sputtered target atoms are 13.

As the implantation energy increases, the electric characteristics of semiconductor devices exhibited noticeable improvement in the wide distribution of dopants. It was, however, difficult to obtain the shallow junction depth. The small and light ions like B caused less lattice damage near the surface even with high implantation energy. However, the nuclear stopping power is more pronounced than the electronic stopping power at the depth of the target material when ion energy is gradually decreased. The concentration distribution difference in the deeper region increases because ions were scattered to sides due to the collisions with lattice damages. On the other hand, heavy ions like As and P cause much lattice damage near the surface.

Fig. 4(a) shows the defect distribution of the initial profile from the result of MD simulation. Fig. 4(b) shows the profile after 10^9 fs. In this simulation, the length recombination is 4? . After ion implantation at 2 x 10^4 ions/cm^2 dose rate, the defects hopping distance is 2.35?. After 10^9 fs, many defects are recombined and vanish. The rate of recombination is dependant to annealing temperature. In high temperature (1500K), the defects (self-interstitials and vacancies) are recombined rapidly as shown Fig.5.

Fig. 6 shows boron and Si damage profiles after 50keV B ion implantation with the dose of $1x10^{11}$/cm^2 using MARLOWE [13]. The dashed lines represent I and V damage distributions. For the low dose implantation, the split between interstitial and vacancy distributions is little. The solid lines represent the distribution of boron after thermal annealing for 15 min at 450℃. A significant fraction of B atoms in the shallow marker are displaced and migrate a considerable distance (~10^2 nm) from their initial positions. Fig. 7 shows 3D distribution of boron after thermal annealing. Table 1 shows simulation parameters. D_I and D_V are the I and V diffusivities, respectively, and E's are the potential energies of simulation particles.

Fig. 8 shows a schematic diagram illustrating the structure of FinFET. FinFET has characteristics such as the ultra thin Si fin for suppression of short-channel effects, two gates which are self-aligned to each other and to the S/D, the raised S/D to reduce parasitic resistance, a short (50nm) Si fin for quasi-planar topography, and the compatibility with low-T, high-k gate dielectrics. Fig. 9 shows a schematic view illustrating the Gunter gird implemented for FDM. Fig. 10 shows the electron density with Vg = 1.5V, 0.5V, and -1.5V. As the voltage ranges 1.5V to -1.5V, the electrons move from the middle of the Si-fin to source and drain.

4 CONCLUSIONS

In this paper, we present our simulation results with basis on an atomistic and quantum mechanical approach. In this work, we employed an MD method for ion implantation process and KMC method for diffusion process, followed by the device simulation. As an exemplary device, the electron density of FinFET with 20nm physical gate length has been investigated.

ACKNOLEDGEMENT

This work was supported partly by the Ministry of Information & Communication (MIC) of Korea through Support Project of University Information Technology Research Center (ITRC) Program supervised by IITA (Institute of Information Technology Assessment), and the author(Ohseob Kwon) would like to express thanks to Mr. Stefan of WSI(Walter Schottky Institute) for fruitful discussion.

REFERENCES

[1] D.Hisamoto, *et al*, IEEE Trans. ED, 47, p.2320 (2000).
[2] L.Chang, *et al*, Tech.Dig.IEDM, p.715 (2001).
[3] B. Yu *et al*, Tech.Dig.IEDM, p.251 (2002).
[4] L.Chang, *et al*, IEEE Trans. ED, 49, p.2288 (2002).
[5] J.Nord, *et al,* Phys. Rev. B (2002).
[6] J. Peltola, *et al*., Nucl. Instr. Meth. Phys. Res. B, (2002).
[7] M. Jaraiz, *et al*., MRS Symp. Proc. 532, 43 (1998).
[8] P. M. Echenique *et al*., Appl. Phys. A 71, 503 (2000).
[9] P. Keblinski *et al,* Phys. Rev. B 66, 4104 (2002).
[10] Martin Jaraiz, Atomistic simulations in Materials Processing.
[11] N.E.B. Cowern *et al*, Phys Rev Lett Vol 69 (1992).
[12] Paola Alippi *et al*, Phys Rev B, Vol 64 (2001).
[13] M.T. Robinson *et al*, Appl. Phys. Lett. 56, 1787 (1990).

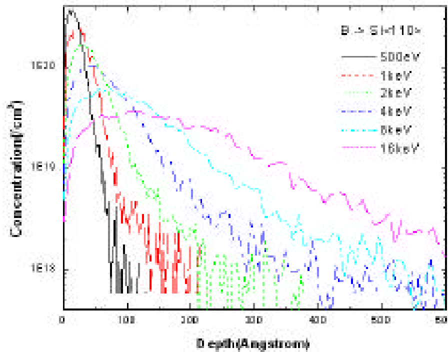

Fig. 1 A plot showing the simulation results with the energy of 0.5, 1, 2, 4, 8, and 16 keV and the dose 1×10^{14}ions/cm^2 B implant.

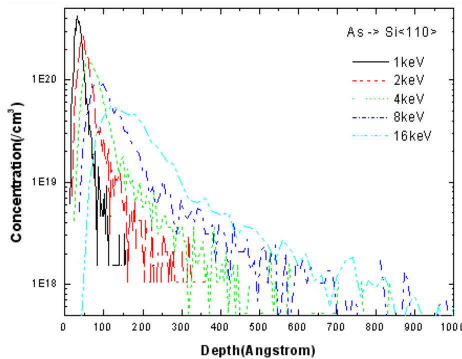

Fig. 2 A plot showing the simulation results with the energy of 1, 2, 4, 8, and 16 keV and the dose 1×10^{14}ions/cm^2 As.

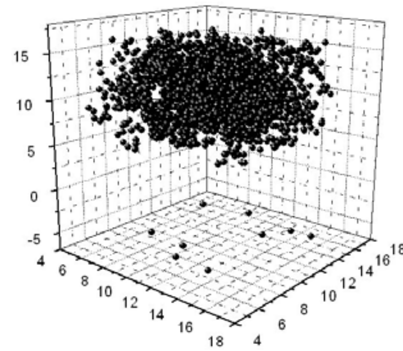

Fig. 3 A plot showing the simulation result with the energy of 5 keV B implant into Si after 4,000 B ions.

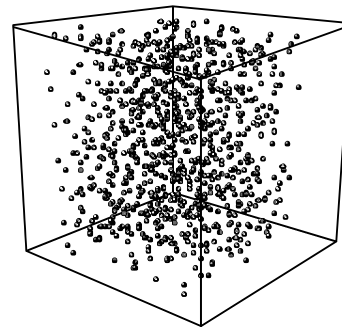

(a)

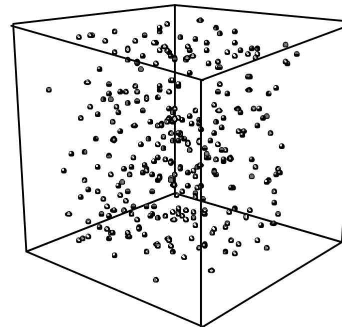

(b)

Fig.4 Plots showing the defect distributions of (a) the initial profile and (b) after 10^9 fs.

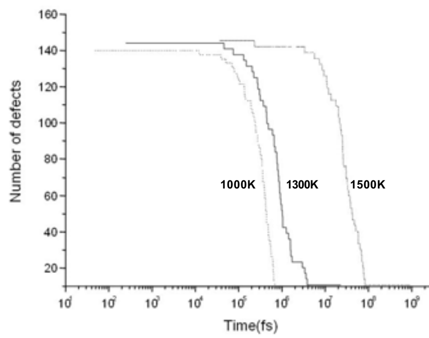

Fig. 5 A Plot showing the number of defects dependent temperature.

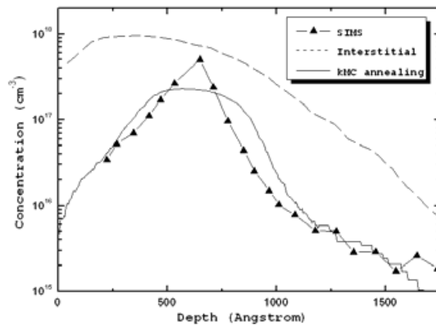

Fig. 6 A plot showing B dopant profile modified by 50keV Si ion implantation to dose of $1\times10^{11}/cm^2$.

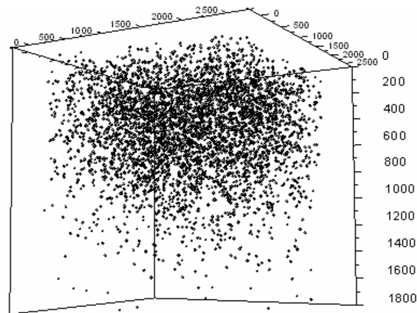

Fig. 7 A plot showing 3D distribution of boron after thermal annealing.

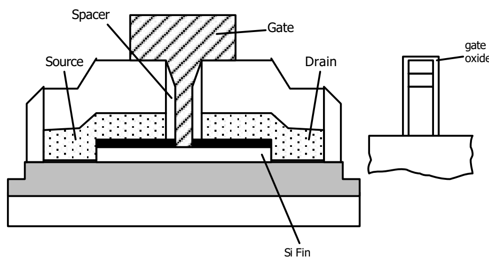

Fig. 8 A Schematic view illustrating FinFET structure.

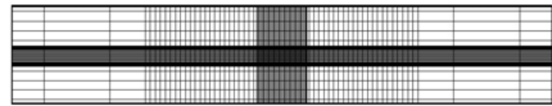

Fig. 9 A Schematic view illustrating the Gunter gird implemented for FDM.

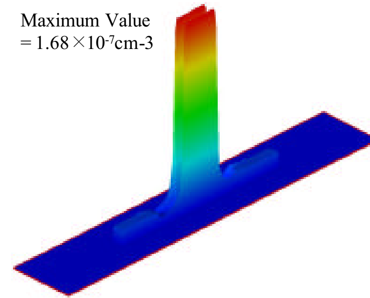

(a)

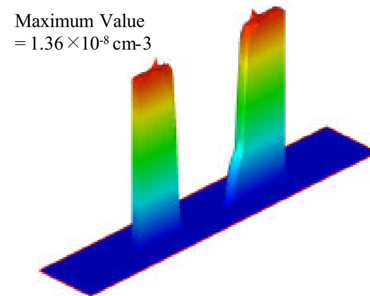

(b)

Fig. 10 Plots showing the electron density with (a) Vg = 1.5V and (b) Vg = -1.5V.

Table 1 Parameters for KMC diffusion.

Diffusivity (cm2/s)		Potential Energy (eV)	
(Single Point Defects : migration)			
D_m_V	1e-3	E_m_V	0.43
D_m_I	5.0	E_m_I	1.0
D_m_B	0.0	E_m_B	5.0
(Interstitial – Vacancy Pair)			
D_m_IV	0.0	E_m_IV	5.0
D_b_IV	0.0	Eb_IV	5.0
D_s_IV	0.0	E_s_IV	0.0
(Interstitial - Boron Pair)			
Dm_IB	1.0	E_m_IB	4.0
D_b_IB	15.0	E_b_IB	1.0
D_s_IB	1e-3	E_s_IB	1.05
(Bi atom)			
D_m_Bi	1.5e-3	E_m_Bi	0.3
D_b_Bi	0.0	E_b_Bi	5